Targeting Mitochondrial RNase P in Heart Failure

Taylor Mattison Billings

A thesis

Submitted in partial fulfillment of the

Requirements for the degree of

Master of Science

University of Washington

2025

Committee:

Rong Tian

Matthew Walker

Patrick Boyle

Program Authorized to Offer Degree:

Bioengineering

University of Washington

Abstract

Targeting Mitochondrial RNase P in Heart Failure

Taylor Mattison Billings

Chair of the Supervisory Committee:

Rong Tian

Department of Bioengineering

Decades of research has shown significant energetic crisis in failing hearts. It has been proposed that impaired mitochondrial biogenesis greatly contributes to energy deficiency and thought to be a pivotal player in disease progression. Strategies aimed at improving mitochondrial biogenesis in failing heart are urgently needed. Previously, we uncovered a significant defect in the processing of mitochondrial RNA in failing heart that is sensitive to the NAD+/NADH redox state. We speculate that downregulation of one of the critical subunits of mitochondrial RNase P, mitochondrial ribonuclease P protein 2 (Mrpp2), is the culprit. Mrpp2 is encoded by the *HSD17B10* gene. It is well known that RNase P is NAD+ dependent, but the exact role of this subunit and its catalytic activity is currently unknown. It has been hypothesized, however, that mrpp2 serves a scaffolding function allowing for the enzymatic activity of the other two subunits: Mrpp1 and Mrpp3. We have found that in cases of reduced Mrpp2 levels, cardiac hypertrophy was present, and methylation of mitochondrial RNA was also downregulated in these hypertrophic cardiac cells. Knowing that downregulation of Mrpp2 levels and the presence of cardiac hypertrophy are closely linked, we hypothesized that the overexpression of the *Hsd17b10* gene would help rescue cardiac health. Using an established murine model of heart failure, we were able to see a restoration of fractional shortening

percentage, a reduction of the left ventricular diameter, and lowered presence of lung edema when delivering a viral vector carrying the *Hsd17b10* gene specifically to failing cardiac muscle, indicating restored cardiac health.

Acknowledgements

I would like to formally thank my PI, Rong Tian and my primary mentor Matthew Walker for their continued help, effort and guidance they have shown to me throughout my development within the program as well as their help on my project. I would also like to extend a thank you to Patrick Boyle for taking the time to join my committee and provide valuable insight to my project and the thesis writing process. Thank you to all the members of the Tian lab as well, without you're continued support and expertise none of this would be possible. Thank you to the American Heart Association, University of Washington (UW) Center for Translational Muscle Research (CTMR), and UW Mitochondrial and Metabolism Center (MMC) for providing the funds needed for this project. Finally, I would like to add a special thank you to all my friends, family, professors, academic counselors, and peers for continuing to support me in my professional and personal development.

Table of Contents

Introduction

Pathogenesis of Heart Failure

Heart failure remains a leading cause of death in the United States and globally[2]. Heart failure is a complex syndrome caused by many pathologic conditions that damage the heart muscle resulting in an inability of the heart to pump sufficient blood to meet the needs of the body[2]. Heart failure is caused by many co-morbidities, with hypertension, ischemic heart disease, diabetes, and cardiomyopathies being the leading causes[3]. Genetic cardiomyopathies are also a common cause of heart failure. The exact cause of cardiac myopathy is unknown, however, the dysfunction of mitochondria transcription/translation as well as electron transport chain (ETC) abnormalities may lead to the failure of mitochondria within heart muscle. There is also evidence that the buildup of reactive oxygen species may lead to oxidative stress and further damage to mitochondria and other cellular components[4].

The onset of heart failure is preceded in most cases by pathologic cardiac hypertrophy or enlargement of the heart. Cardiac hypertrophy results in an increase in cardiomyocyte size and genetic reprogramming of metabolism, calcium signaling, protein synthesis, and gene transcription[5]. Cardiac metabolism reverts to a more fetal like state relying more on glucose utilization and ketone catabolism over fatty acid oxidation[6]. Initially, the hypertrophic response is adaptive but over time becomes maladaptive and the heart ultimately fails. Heart failure is associated with altered energy metabolism and failing heart is often referred to as an "engine out of fuel"[2, 7]. Failing hearts have been shown to have up to 30% less ATP content than healthy hearts[8]. It appears mitochondrial oxidative metabolism is the culprit, but the exact mechanisms are still heavily debated[2]. Impaired mitochondrial function in failing heart is multifaceted. It can occur due to dysregulated transcriptional and translational processes that regulate both nuclear

DNA (nDNA) encoded and mitochondrial DNA (mtDNA) encoded mitochondrial protein expression[9-11]. Altered NAD+ biosynthesis and imbalanced NAD+/NADH redox have also been implicated in causing mitochondrial dysfunction in failing heart[11-13]. Imbalanced redox can lead to alterations in post-translational modifications of mitochondrial protein such as hyperacetylation due to sirtuin inactivity. Calcium overload and high reactive oxygen species (ROS) can also compromise mitochondrial integrity and function. It is clear from decades of research that mitochondrial dynamics/biogenesis and metabolism are severely altered in failing heart[9, 14]. Decades of research has shown significant energetic crisis in failing hearts. It has been proposed that impaired mitochondrial biogenesis greatly contributes to the energy deficiency and thought to be a pivotal player in the disease progression. Strategies aimed at improving mitochondrial biogenesis in failing heart are urgently needed.

Mitochondria biogenesis is impaired in the failing heart, which often is attributed to the downregulation of the nuclear transcription factor peroxisome proliferator-activated receptor γ coactivator alpha (PGC-1α)[9, 10]. However, it was found that PGC-1α downregulation does not account for decreases in the expression of mitochondrial DNA (mtDNA) encoded proteins in human failing heart, and moreover, promoting PGC-1α driven mitochondrial biogenesis in animal models of HF does not rescue the mitochondrial dysfunction or improve the outcome[10, 11]. Recently, we uncovered a significant defect in the processing of mitochondrial RNA in failing heart that is sensitive to the NAD+/NADH redox state[11]. We hypothesize that downregulation of one of the critical subunits of mitochondrial RNase P, mitochondrial ribonuclease P protein 2 (Mrpp2), is the culprit. Mrpp2 serves a scaffolding function in the RNase P splicing complex that allows subunit 1 (Mrpp1) to methylate mitochondrial precursor transfer RNA and subunit 3 (Mrpp3) to cleave the 5’ end of precursor transfer RNA releasing the

adjacent mature messenger RNAs (mRNA). The mature messenger RNA (mRNA) encodes the thirteen ETC proteins responsible for mitochondrial oxidative phosphorylation. We plan to test our hypothesis by replenishing Mrpp2 levels in pathologic cardiac hypertrophy and determine if mitochondrial RNA methylation and RNase P activity is restored.

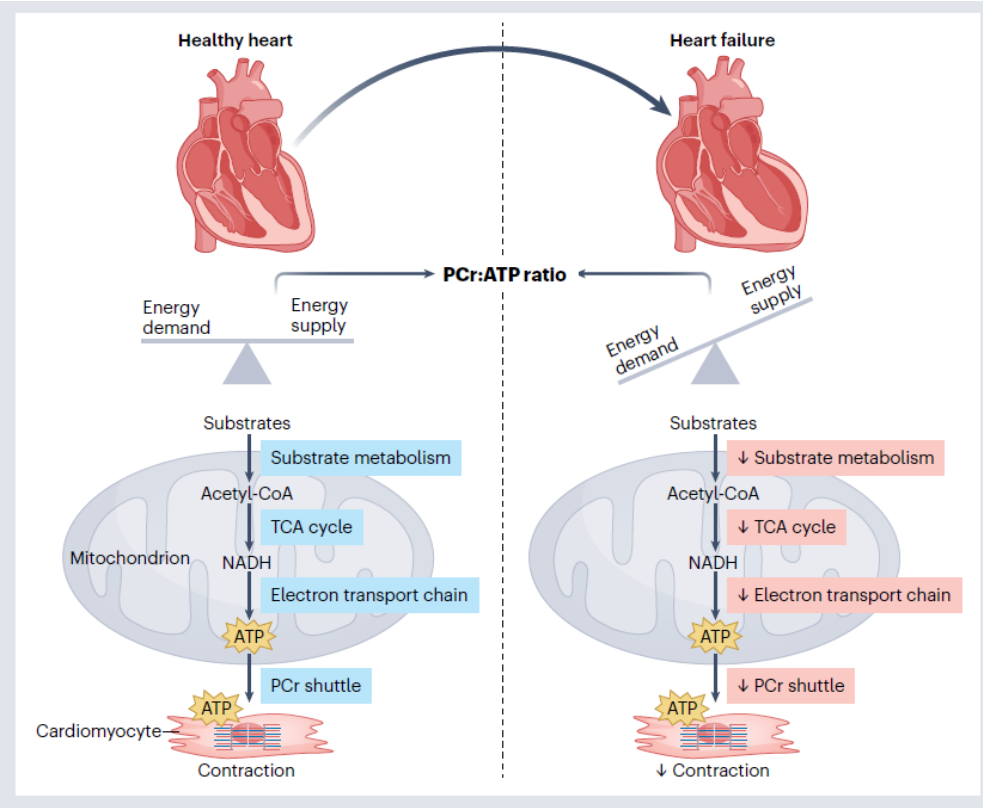

Figure 1: The balancing act between energy supply and demand in heart function and mitochondrial factors that contribute to keeping supply up with demand[5].

Mitochondria structure and function:

The mitochondrion is a double membraned organelle essential for energy production in eukaryotic cells[2]. Most energy requirements for mammals are met by catabolism of carbohydrates and fatty acids to produce adenosine triphosphate (ATP). ATP powers many reactions throughout the body including muscle contraction and relaxation[14]. Oxidative metabolism supplies 90% of the ATP needed for muscle contraction and requires a constant supply of oxygen and carbon fuel sources such as glucose, fatty acids, ketones, and amino acids[15-17]. The outer mitochondrial membrane (OMM) is composed of a lipid bilayer and contains specific channels that allow diffusion of molecules into and out of the mitochondria. The inner mitochondrial membrane (IMM) and OMM of mitochondria are separated by the intermembrane space (IMS)[18]. The IMS plays a role in oxidative phosphorylation as protons build up in the IMS creating a proton gradient established across the IMS and the mitochondrial matrix. The inner membrane is a folded complex called cristae which is essential for increasing the surface area of the membrane for reactions involved in oxidative phosphorylation. The mitochondrial respiratory complexes are in the mitochondrial cristae forming the ETC[19]. There are four ETC complexes (I-IV) that pump protons out of the mitochondrial matrix into the IMS. The protons then diffuse back through the inner membrane via ATP synthase (Complex V) thereby coupling electron transfer through ETC for ATP synthesis[20]. The matrix is the innermost space of the mitochondrion. The matrix contains soluble protein, ribosomes, and the mtDNA[21]. Enzymes that are crucial for beta fatty acid oxidation and citric acid cycle are contained in the mitochondrial matrix. The citric acid cycle produces NADH and FADH2 energy carriers that are oxidized by the ETC protein for ATP synthesis[22].

For energy yielding reactions to proceed the mitochondrial proteome must be constantly maintained by both nuclear and mitochondrial specific factors. Proper transcription and translation of the mtDNA is required for oxidative ATP production in the heart[23].

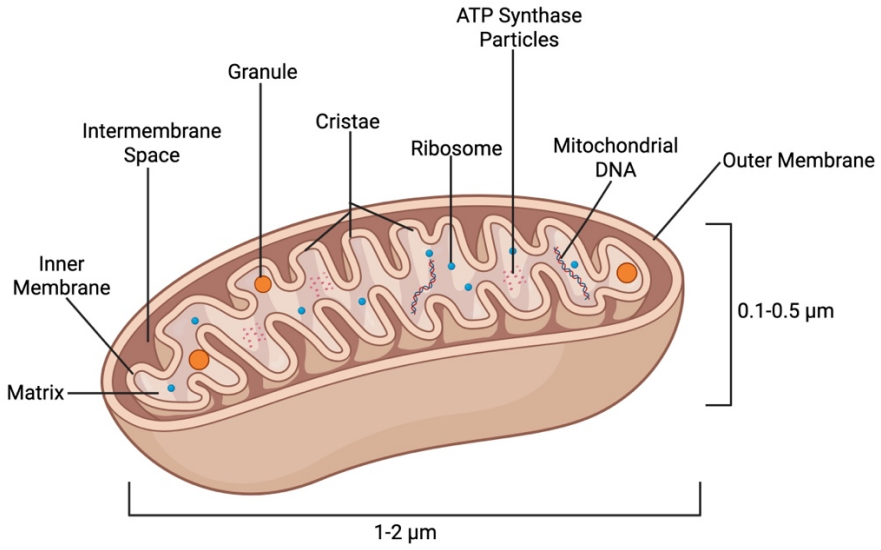

Figure 2: Structure of mitochondria.
Created in BioRender. Billings, T. (2025) https://BioRender.com/y4qnrwm

Mitochondrial genome transcription:

Mitochondria are constantly in need of new proteins that allow them to function. As mentioned above, mitochondria have their own genome, however, 95% of the genes needed for synthesis of mitochondrial proteins are encoded by the nDNA[24]. Nuclear-encoded mitochondrial proteins that are synthesized via the nuclear genome include intermembrane space, matrix, outer, and inner membrane proteins as well as all the transcription factors used in mitochondrial gene expression[25]. Proteins destined to locate to mitochondria contain mitochondrial localization sequences (MLS) that allow for import into the mitochondria after

synthesis in the cytosol. MLS are short peptides that are around 15-70 amino acids long and positively charged located on the N-terminus of proteins. The MLS is cleaved upon entry into the mitochondrial matrix by mitochondrial processing peptidase (MPP). The small mitochondria genome encodes for 13 proteins, 2 rRNAs, and 22 tRNAs that are needed for mitochondrial respiratory function. The process of transcription in the mitochondrial genome starts at the L-strand (LSP) and H-strand (HSP) promoters within the major non-coding region of the genome. Transcription of mtDNA occurs when the cell needs to respond to differing energy and metabolism demands[26]. Transcription of the mitochondrial genome is initiated by mitochondrial RNA polymerase (POLRMT), an enzyme responsible for transcribing mitochondrial DNA (mtDNA) into RNA. To ensure proper execution of the transcription process, coordinated action of transcription factor A (TFAM) transcription factor B2 (TFB2M), transcription elongation factor (TEFM) and transcription termination factor (MTERF1) are necessary. To begin transcription, the POLRMT associates with the TFB2M and TFAM transcription factors which catalyzes the transcription events[27]. TFAM works by binding to the DNA and packaging the DNA in the nucleoid of the mitochondria. The TFB2M then works to melt the DNA at initiation and modifies the structure of the POLRMT to open the promoter. This then begins the elongation phase of transcription[28]. For elongation to occur, TEFM must be present. This transcription factor protein increases the affinity of POLRMT to the DNA. This affinity allows for the RNA polymerase to stay attached to the DNA and appropriately synthesize the correct base pairs for messenger RNA that will be later used in translation and the synthesis of the proteins needed by the mitochondria[29]. The final step of transcription is the termination step. The exact mechanisms of this process are still unclear within mitochondria; however, it has been found that MTERF1 plays a role in this process. Evidence from various studies has led to a belief that

MTERF1 binds to a termination site on the mtDNA and blocks the polymerase from synthesizing more mRNA and therefore the chain is released for the RNA processing step which we discuss below[27].

Mitochondrial RNA Processing

Expression of the mitochondrial genome is a tightly regulated process that relies on post-transcriptional RNA processing. In the mitochondrial genome, RNA is transcribed into a long premature polycistronic RNA transcript[30]. This transcript includes all 13 protein coding genes that are necessary for synthesizing components of the electron transport chain along with an additional 24 genes that encode for tRNAs and rRNAs[31]. This transcript is organized in a way that the tRNA genes are interspersed between the other protein coding and rRNA genes within the transcript. This model allows the tRNAs to act as spacers that separate adjacent coding sequences and allows for efficient processing of the individual transcripts within the chain. This model is what is often referred to as the tRNA punctuation model[32]. For the mature genes to be translated into protein the tRNA punctuations must be excised[33]. Two enzymatic complexes are responsible for cleaving the tRNAs from the polycistronic RNA. Mitochondrial RNase P cleaves the 5' end and RNase Z cleaves the 3' end[34].

Mature mitochondrial tRNAs (mt:tRNAs) are crucial for both the translation step and the maturation of the other RNA transcripts from which the tRNA originated from. Mature mt:tRNAs must be folded into a cloverleaf structure containing a D-loop and anticodon loop, a structure that is necessary for translation of the genome[35]. Improper processing at the 5' end of the immature tRNA can lead to misfolding of the molecule which will impair the ability of mt:tRNAs to recognize codons and deliver amino acids necessary for creating proteins[36]. As a result, any defections within the processing of tRNAs can compromise the translation of the

mitochondrial genome into proteins necessary for the ETC and thus lead to mitochondrial defects[37]. Mitochondrial RNase P plays a crucial role in the initiation of tRNA maturation and better understanding its function, regulation, and possible defects can help in maintaining gene expression and bioenergetic homeostasis of patients with energetic imbalance due to defective mitochondria[38].

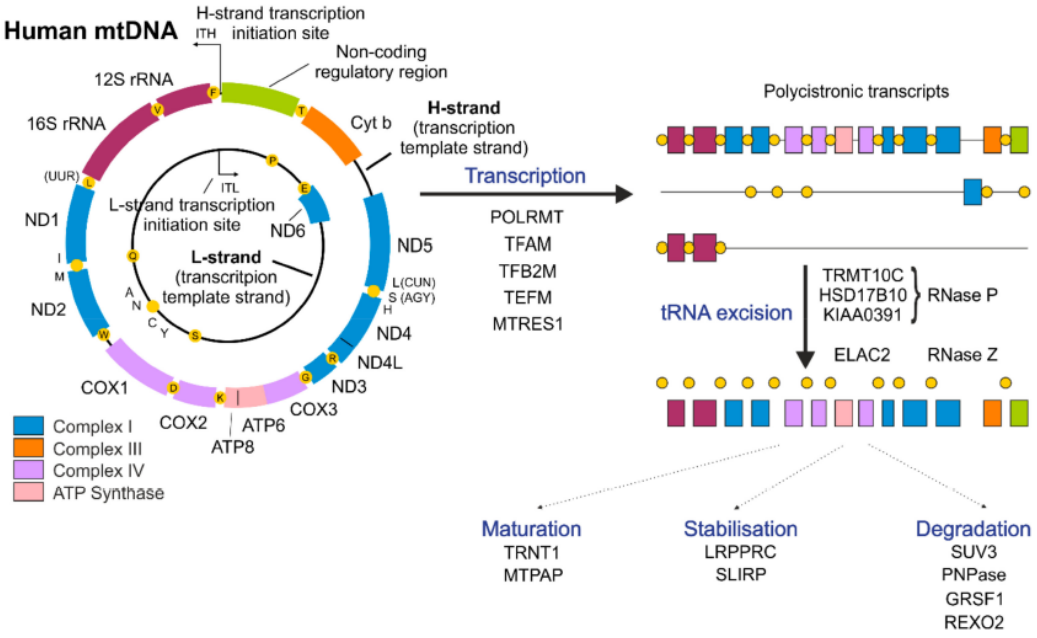

Figure 3: On the left is the human mitochondrial genome before processing. The top right shows the raw polycistronic transcript before excision. The bottom right shows the transcript post excision of tRNAs[33].

Structure of Mitochondrial Rnase P

The mitochondrial RNase P complex in mammals is unique in that it is made up of a complex of three protein subunits (Mrpp1, Mrpp2, and Mrpp3)[39-41]. Mrpp1 or tRNA methyltransferase 10 homolog C (Trmt10c) is responsible for the N^1-methylation if adenosine and guanosine at position 9 in mitochondrial tRNAs[42]. This step is crucial to form a stable tRNA that can properly decode mRNA sequences during translation. The exact role of Mrpp2 also called short-chain dehydrogenase/reductase 5c1 (Sdr5c1) in the RNase P complex is unknown, however, it is hypothesized that it may act as a scaffolding protein important for the methylase function of Mrpp1 and the endonuclease activity of Mrpp3. Mrpp3 also called Protein Only RNase P Catalytic Subunit (Prorp) is responsible for cleaving the 5' end of precursor mitochondrial tRNAs from the immature RNA releasing the mature coding RNA and tRNA[43].

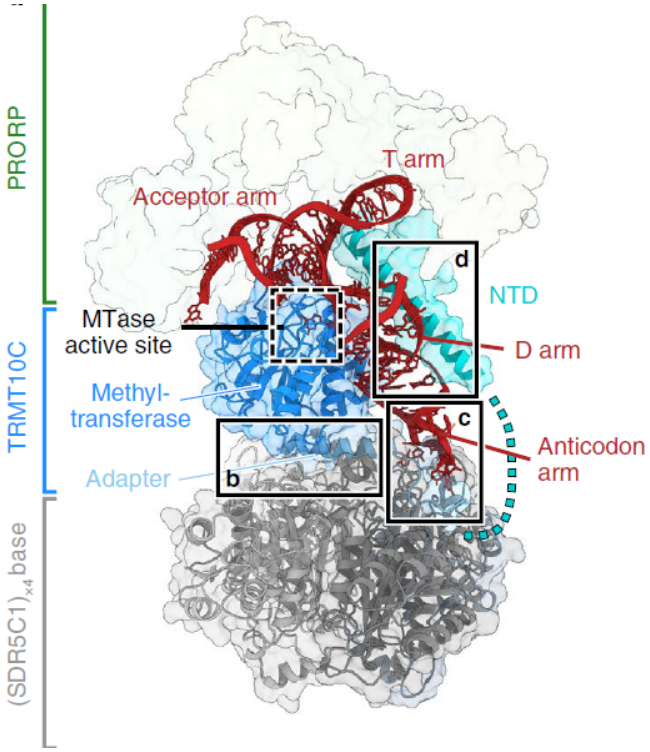

Figure 4: 3D depiction of human mitochondrial RNase P[40]

Role of RNase P in Disease

The proper functioning of mitochondrial RNase P is crucial for the post-transcriptional processing of mitochondrial RNAs. Faults in RNase P complex have been linked to primary mitochondrial disease indicated by severe impairment in energy production and early death[34]. Patients with dysfunctional RNase P experience developmental delays, neurological disorders, cardiomyopathy, and metabolic abnormalities. In severe cases, these defects can be fatal[44]. There are several diseases that are due to the dysfunction or absence of subunits in the RNase P complex. Missense mutations in the *TRMT10C* gene encoding MRPP3 disrupt the normal processing of tRNAs, impairing the rate at which ETC proteins are produced[45]. Affected patients experience developmental delays, liver dysfunction, respiratory complexities, hypotonia, feeding difficulties, and cardiomyopathy. Mutations in *TRMT10C* lead to early infantile death due to the failure of mitochondria and insufficient energy production[46].

Among the subunits of mitochondrial RNase P, the subunit that is most often linked to severe disease is MRPP2. These diseases are often fatal and especially prevalent in infants and young children. The severity and manifestations of the disease vary depending on the mutation found within the *HSD17B10* gene, which encodes the Mrpp2 protein[47]. Mutations that disrupt MRPP2 tetramerization and the catalytic activity of the mtRNase P complex are most severe[34]. The patients have impaired 5’ cleavage of mitochondrial tRNAs and decreased synthesis of mitochondrial proteins[34]. Clinical symptoms within these patients include loss of cognitive function, cardiomyopathy, epilepsy, blindness, and neurodegeneration. Due to the lack of

sufficient energy production within mitochondria, patients usually succumb to the disease, often in early childhood[47].

One such disease that arises due to mutations in the *HSD17B10* gene is HSD10 disease. This disease is an X-linked neurodegenerative disorder with detrimental effects on muscle, vision, neurological communications, and the heart. HSD10 disease is associated with the *HSD17B10* gene which is located on the X chromosome. Since males only have one X chromosome, they are more severely affected by the disease and likely will not live past childhood[48].

Mutations within the Mrpp3 subunit of human mitochondrial RNase P has been linked to biallelic *PRORP* mutations. These mutations primarily affect the processing of mitochondrial tRNAs and lead to a diminished processing of the mitochondrial genome[49]. Individuals who are affected present a large array of symptoms including developmental delay, hearing loss, hypotonia, insulin resistance, seizures and cardiomyopathy[34, 49]. Perrault syndrome is an example of a disease that has links to mutations within the Mrpp3 subunit which in turns causes mutations in proteins synthesized from the mitochondrial genome. In severe cases, the dysfunction of Mrpp3 can be fatal to the patient[34].

AAV Vector for gene therapy in heart muscle

Adeno-associated virus (AAV) is used as a delivery mechanism of functional genes into cells to treat diseases[50]. AAVs are made up of a protein shell which surrounds a small, single stranded genome. This genome is then delivered into target cells to express the genes they carry[51]. To deliver the gene into cells, the virus must first bind to specific cellular receptors and co-receptors that initiate endocytosis. Once the vector is inside the cell, the viral particle is brought to the trans-Golgi network. Once inside the nucleus, the single DNA is converted into double-stranded DNA and expression of the recombinant genome can occur[52]. AAV therapies are being investigated as treatments relating to a variety of diseases including cancers, neurological diseases, blood diseases, immune diseases, and cardiovascular diseases[53]. Adeno-associated virus serotype 9 (AAV9) has shown to increase viral delivery to cardiac muscle and can enhance the delivery of genetic material to myocardium[54].

Gene therapies could provide new innovative treatment for heart failure. AAVs are effective and have potential to be less invasive than other types of heart therapy. Recently, clinical trials have been conducted testing the effectiveness of AAV gene therapies in treating hyperlipidemia, cardiac amyloidosis, and heart failure[55]. Infusion of AAV/SERCA2a into patients with heart failure was beneficial and no safety concerns or negative effects were noted in the patients receiving the AAV gene therapy[56]. Similarly, viral gene therapies using rAAV9 have helped reverse the effects of cardiomyopathy by improving cardiac capacity, improving skeletal muscle function, aiding in cardiac regeneration, and reducing cardiac hypertrophy[53]. By using information from past pre-clinical studies and AAV research we have designed a novel AAV to deliver the *Hsd17b10* gene specifically to heart muscle with the aim of improving mitochondrial RNA processing in failing heart.

Hypothesis and Aims

We **hypothesize** that reduced Mrpp2 protein level in failing hearts causes impairment of mitochondrial biogenesis and function and that replenishing Mrpp2 levels rescues the heart failure phenotype by improving RNase P splicing complex activity. Therefore, we propose the following aims to test the hypothesis:

Aim 1: To test the hypothesis that pathologic cardiac hypertrophy causes downregulation of the *Hsd17b10* gene and impaired mitochondrial RNase P activity in differentiated H9c2 cells.

Aim 2: To test if replenishing Mrpp2 levels in failing heart improves mitochondrial RNase P activity *in vivo* and rescues the heart failure phenotype.

Materials and Methods

Animal Care and Mice used

All procedures involved were approved by the Institutional Animal Care and Use Committee of the University of Washington. Wildtype C57BL/6 mice were purchased from Charles River Laboratories. All mice used were housed at 22C with a 12-hour light and a 12-hour dark cycle with access to water and chow. Male mice were used throughout this study.

Transverse Aortic Constriction Surgery

Male mice underwent transverse aortic constriction (TAC) or SHAM surgery in order to induce hart failure through pressure overload. Mice were anesthetized with an intraperitonial injectioon of 130 mg/kg of ketamine and 8.8 mg/kg of xylazine in saline. After the administration of anesthesia, the mice were intubated with a 20 gauge cannula and ventilated 140 breaths per minute by a small-animal TOPO ventilator (Kent Scientific). The aortic arch was then exposed through a left thoractomy and separation of the thymus. The transverse aorta was constricted by tying a 6-0 Ethilon ligerature against a 27-gauge blunt needle around the aorta. The needle was quickly removed after this step and the skin and chest region were closed woth a 5-0 polypropylene suture. After surgery, the mice were removed from ventilation and placed on a heating pad while they recovered. Sustained release buprenorphine (0.5 mg/kg) was subcutaneously administered for analgesia. The SHAM operated mice underwent all the same procedures as the TAC operated mice besides the aorta constriction. This is to ensure that any complications are not from surgical practices. All mice were monitored every 12 hours for the first 72 hours of surgery with daily visits for the following 4 weeks post-operation.

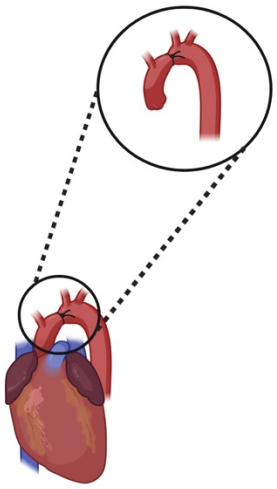

Figure 5: Diagram of TAC surgery with constriction of the aorta.
Created in BioRender. Billings, T. (2025) https://BioRender.com/swfng7o

Retroorbital Injection of AAV9s

Hsd17b10 cDNA and GFP were separately cloned into ITR-containing AAV9 plasmid harboring the chicken cardiac TNT promoter to yield constructs AAV9.cTnT.Mrpp2 and AV9.cTnT.GFP, respectively. The AAV9 production and quality control was done by the Penn Vector Core. AAV9 virus (1×10^{12} virus genome per animal) was injected the mice and their control littermates by retro-orbital injection under isoflurane.

Mouse Heart Harvest

All procedures involving animal use were approved by the Institutional Animal Care and Use Committee of the University of Washington. All mice were housed at 22 °C with a 12-hour light, 12-hour dark cycle with free access to water and standard chow. Male mice were used for experiments in this study. Mice were anesthetized by intraperitoneal injection with sodium pentobarbital and weighed. The heart was promptly removed from the chest cavity and washed in cold PBS. The heart was then drained of any blood and the any remaining aorta, fat and lung was removed from the heart. The heart was then weighed and clamped with a flash frozen clamp

and stored in liquid nitrogen. Once all hearts and organs were harvested, the heart tissue was stored in -80ºC until further analysis was performed.

Heart Weight/Body Weight (HW/BW) Ratio

This ratio is used to help assess cardiac hypertrophy in the mouse models. A normal heart HW/BW ratio around 4-5 mg/g, with elevated levels indicating pathological hypertrophy due to the heart being heavier than normal. This ratio is calculated by weighing both the whole-body weight of the mouse and just the weight of the heart and dividing the heart weight by the body weight. This tells how much of the total body weight comes from the heart.

Lung Edema (Tissue Wet/Dry Ratio Measurement)

A weigh boat was labeled with permanent marker and placed into a drying oven for 4 hours. The weigh boat was handled carefully with tweezers. After the 4-hour time, the weigh boat was pulled from the oven with tweezers and weighed. This weight was recorded as W1. A 20-40 mg piece of lung tissue was then harvested from male mice and blotted dry with tissue paper and weighed on the labelled weigh boat. This measurement was recorded as W2. The weigh boat and tissue were then placed into the drying oven for 72 hours at 56ºC. After 72 hours, the tissue and weigh boat were measured together, and the weight was recorded as W3. To determine the dry/wet ratio, the calculation is as follows: (W2-W1)/(W3-W1).

Western Blot Sample Preparation

Preparation of Lysate (Heart Tissue)

Eppendorf tubes were prepared with 1 volume of 0.5mm homogenization beads. RIPA buffer was then prepared by adding 1 protease inhibitor tablet to 25 mL RIPA. Once RIPA+PI buffer was prepared, 250 µl of the mixture was added to the 1.5 mL tubes and placed on ice for 10 minutes. After 10 minutes, 20-30 mg of heart tissue extracted from male mice was added to the RIPA+PI buffer in the 1.5 mL tubes. The sample tubes were then placed into a "bullet blender" and homogenized for 5 minutes at the maximum speed of the unit. An additional 250 µl of the RIPA+PI buffer was then added to the sample tubes and vortexed for 15 seconds. The samples then sat on ice for 30 minutes. After 30 minutes on ice, the samples were centrifuged at 10,000 g at 4ºC for 20 minutes. After centrifuging, the supernatant was transferred to a new 1.5 mL Eppendorf tube and mixed via pipet. 5 µl of this supernatant was then added to 55ul of di H_2O for protein assay.

Cell Harvesting (Adherent Cells)

On ice, cold media was aspirated off cells and cold PBS was added to each well to wash the cells. PBS was aspirated and the process repeated. Ice cold lysis buffer (RIPA with fresh protease inhibitors) was added to each well of the cell plate at a volume of the plate size in cm x 0.018/cm^2. The plate was incubated at 4ºC for 30 minutes with a gentle rocking motion then scraped from the surface using a rubber spatula. The cells were then transferred to a microfuge tube and spun for 10 minutes at 12,000 RPM at 4ºC. Supernatant was transferred to a fresh tube and a BCA protein assay was performed.

BCA Protein Assay

Protein concentration was determined using the Pierce ™ BCA Protein Assay Kit. Standards were first prepared in 1.5 mL Eppendorf tubes according to the following table:

Vial	Volume of Diluent (µl)	Volume and Source of BSA (µl)	Final BSA Conc. (µg/mL)
A	0	300 of Stock	2000
B	125	375 of Stock	1500
C	325	325 of Stock	1000
D	175	125 of vial B dilution	750
E	325	325 of vial C dilution	500
F	325	325 of vial E dilution	250
G	325	325 of vial F dilution	125
H	400	100 of vial G dilution	25
I	400	0	0=Blank

Reagents A and B were then mixed in a 50:1 ratio in a 15 mL conical tube to create working reagent. 25 µl of sample or standards were then added to a well plate followed by 200 µl of working reagent into each well containing sample or standard. The plate was than incubated for 30 mins at 37ºC. After incubation, protein concentration was read at 562 nm.

Preparation of Loading Samples

Samples were prepared in Laemmli buffer at a 1:1 ratio. 200 µl of sample and 200 µl of buffer were added to a new 1.5 mL Eppendorf tube and stored at -20ºC for western blot analysis. The amount of protein to be added to the well was calculated based on results from a BCA protein assay.

Western Blot Analysis

Electrophoresis and Protein Transfer

Samples were loaded and ran on a 10% SDS-PAGE gel for 20 minutes at 75V then changed to 100V and ran until the dye reached the bottom. The entire run took around 2 hours. When the electrophoresis portion was finished, the gel was placed in an electroblotting cassette along with transfer buffer. The equipment was then place in a bucket of ice to prevent overheating during the transfer process. The gel was then transferred onto the membrane for 1 hour at a constant current of 110V. When the transfer was complete, the cassette was disassembled and the membrane was placed in ponceaus stain for about 10 minutes, rinsed, then a scan of the membrane was taken via a scanner.

Antibody Detection

The membrane was washed with TBST for 5 minutes then blocked with BSA for 1 hour. After 1 hour, the primary antibody that was diluted in TBST was added onto the membrane and incubated overnight at 4ºC with gentle agitation. The following day, the membrane was then washed 3 times with TBST for 5 minutes each then the diluted secondary antibody was added. The secondary antibody was left on the membrane with gentle agitation at room temperature for 1 hour. ECL was then added to the membranes for 2 minutes to allow for signal detection. The membranes were then imaged and put into ImageJ for further analysis.

Echocardiography

Using the ultrasound system

Mice were subject to isoflurane anesthesia to reduce motion but sustain cardiac function to around 400-450 bpm. The mouse was first sedated in a chamber and then restrained on a heated stage with a continuous flow of isoflurane. Body temperature, ECG and respiratory monitoring was used to prioritize the safety of the mouse as well as keeping consistency among all the subjects. Hair removal was then applied to the chest and removed after a few minutes to remove hair from the chest region. Ultrasound gel was then placed on the chest and the probe was positioned over the heart to find papillary muscles using B-mode. Once the papillary muscles of the left ventricular were identified, the machine was switched to M-mode to take video of the systole and diastole function within the left ventricular. After measurement, the mouse was cleaned off and removed from isoflurane and placed back in their cage.

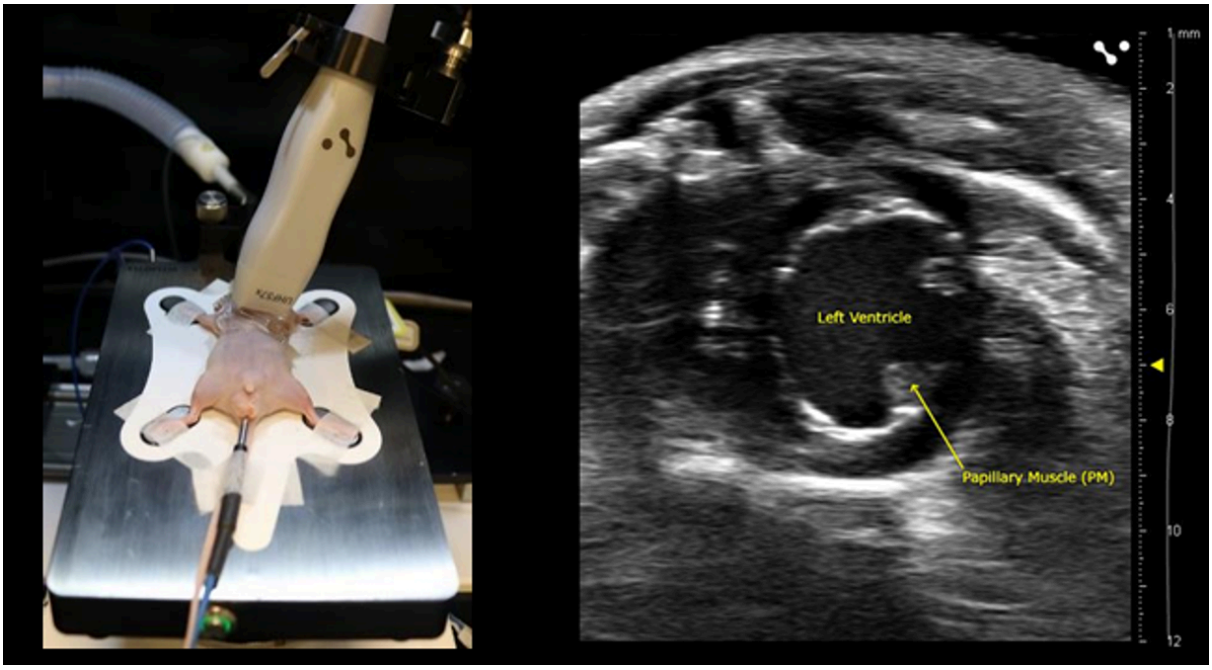

Figure 6: Diagram of echocardiography setup on the left and B-mode photograph on the right. [1]

Fractional Shortening (FS%)

To assess contractional functionality of the left ventricular, the fractional shortening percentage was collected for each mouse. Measurements of the left ventricle were taken in M-mode echocardiography. Fractional shortening measures contractility by comparing how much the left ventricular decreases during systole in comparison to diastole. When analyzing a frozen picture in m-mode, the left ventricular internal diameter at end diastole and the left ventricular internal diameter at end systole are measured. The fractional shortening was assessed using the following formula: $\left(\frac{LVIDd-LVIDs}{LVIDd}\right)x100$. A normal FS% for mouse is 30-40%.

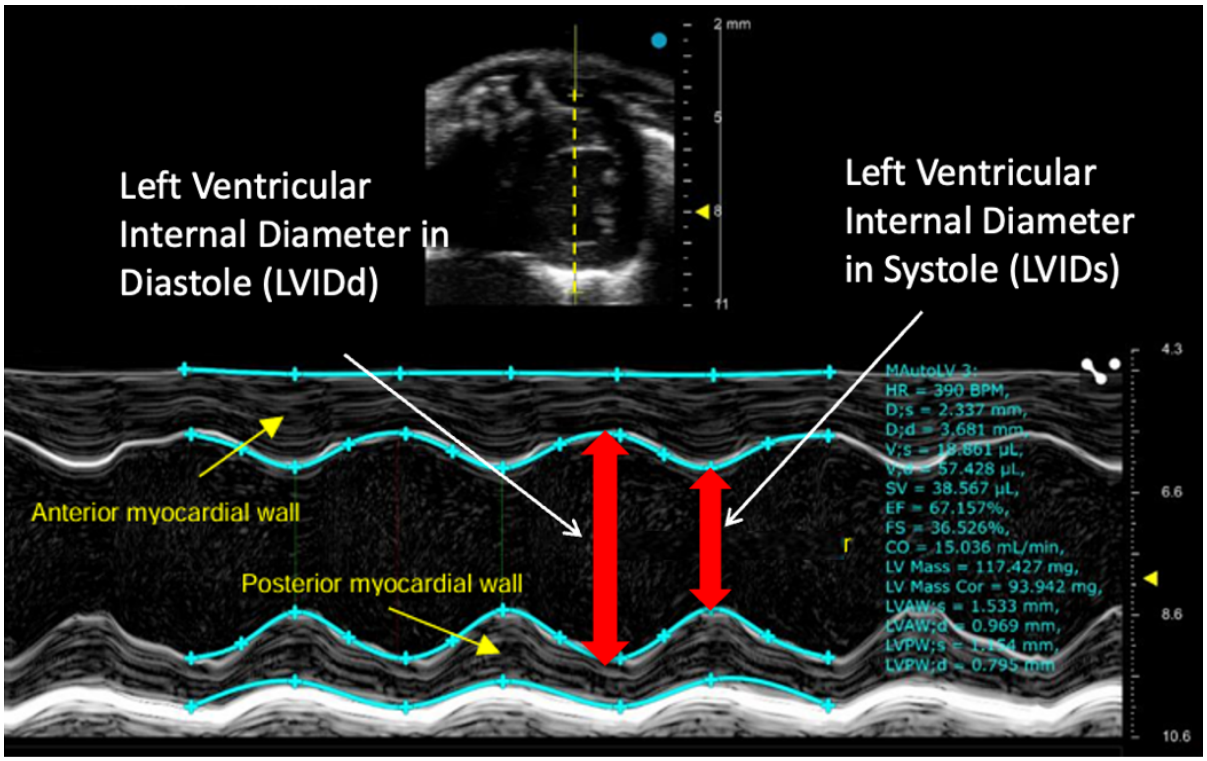

Figure 7: M-mode echocardiography snapshot indicating FS% measurements.[1]

Left ventricular Internal Diameter in Diastole LVID:d

To assess the LVID:d, the measurement of the distance between the distance from the endocardial edge of the septum to the endocardial edge of the posterior wall was measured in millimeters from a still image in M-mode. This was measured over 3 cycles and averaged. This measurement is taken when the ventricle is most expanded and filled with blood. LVID:d is measured to assess how dilated the left ventricle is and to assess cardiac function. The normal range for mice is around 2.5-3.5mm.

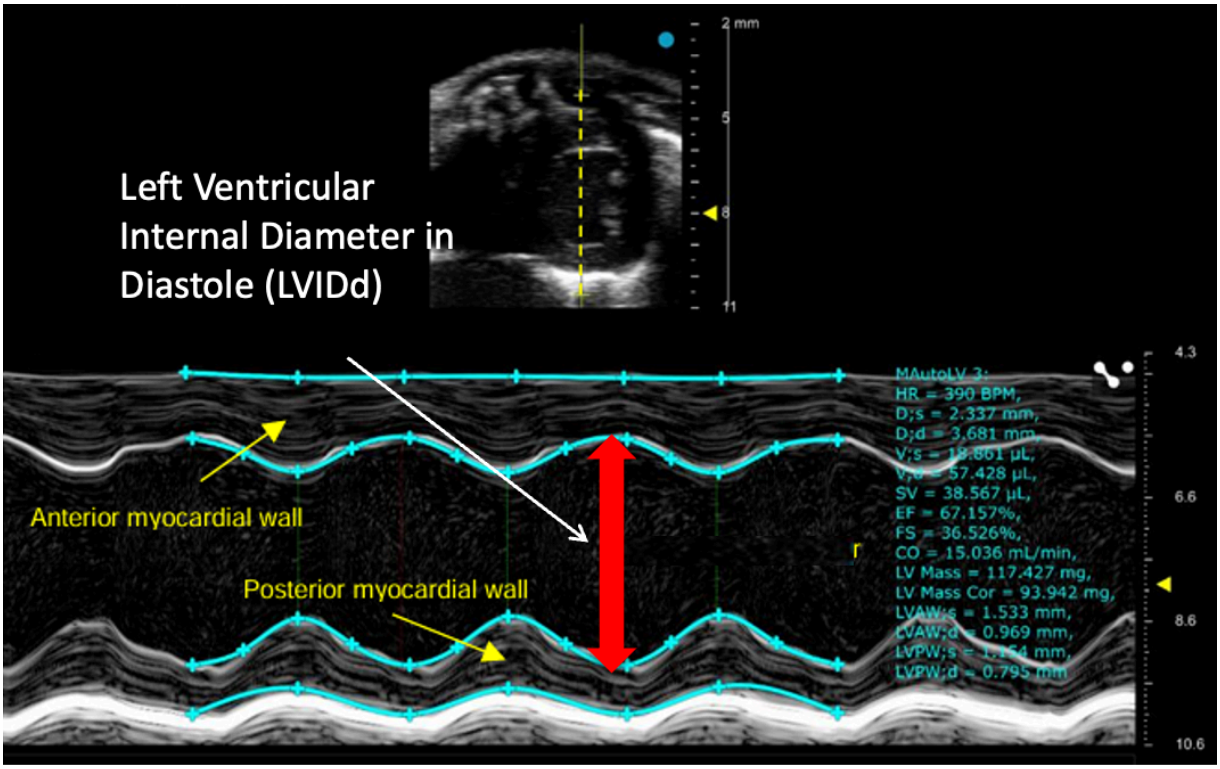

Figure 8: M-mode echocardiography snapshot indicating LVID:d measurements.[1]

Quantitative Polymerase Chain Reaction (qPCR)

RNA Extraction

Small (10-30mg) pieces of frozen heart tissue were placed in a cold 1.5 mL microcentrifuge tube. 600 µl of lysis buffer (LB) was then added to the microcentrifuge tubes, followed by 0.2 mg/mL proteinase K. This step was crucial to degrade the proteins in the tissue. The samples were then incubated at 55ºC overnight. The next day, 100 ug/mL of RNase Awas added to the tubes to degrade the RNA in the samples. The samples were then incubated for another 30 minutes at 37ºC. After incubation, 250 µl (7.5 M) of ammonium acetate and 600 µl of isopropanol (0.7 v/v) were added and the solution was mixed well to give a visual DNA structure. The samples were then centrifuged at 15,000xg for 10 min at 4ºC and the supernatant removed. Pellets were then washed with 500 µl of 70% ethanol and the pellets were dried. After the pellets dried, they were resuspended in 100 µl of TE buffer. Once resuspended, the concentration of the samples was read on a nanodrop and diluted to 10 ng/ DNA/ul with double-distilled water. The samples were then ready for qPCR.

Quantitative PCR

Primers that were used for analysis were identified and the appropriate forward and reverse primers were diluted to a stock concentration of 100 µM with double-distilled water. Each gene was then prepared into a working stock master mix of forward and reverse primers to have a concentration of 10 µM each. In PCR tubes, a total volume of 5 µl of the following components were added each gene: 2 µl DNA, 3 µl Syber green mix +forward/reverse primers (2.5 µl and 0.5 µl respectively). The tubes were then spun down at a high speed and put into a thermocycler under the following conditions: 95ºC for 5 min (preamplification). 45 cycles of

95ºC for 10 seconds, 60ºC for 10 seconds, and 72ºC for 20 seconds (amplification step). A melting curve was then identified to confirm PCR products using a fluorescence acquisition of 95ºC for 5 seconds, 66ºC for 1 minute, and a gradual increase of temperature to 97ºC.

Differentiating H9C2 Cells

Differentiation of H9C2 cells was induced at 80-90% confluence. Cells were harvested using 2 mL of a trypsinization solution (4.5 mL PBS + 0.5 mL trypsin). Cells were then pelleted using centrifugation (1,200 rpm, 3 min) and the supernatant removed. Cells were resuspended in regular growing medium (10% FBS DMEM) and counted so the cells were plated in 10 cm plates at a final density of 100K/mL. After incubating at 37ºC for 48-hours, differentiation was induced by changing the medium to 1% FBS DMEM and 1 µM retinoic acid for 5-7 days. Differentiation was confirmed using troponin markers in western blot assay.

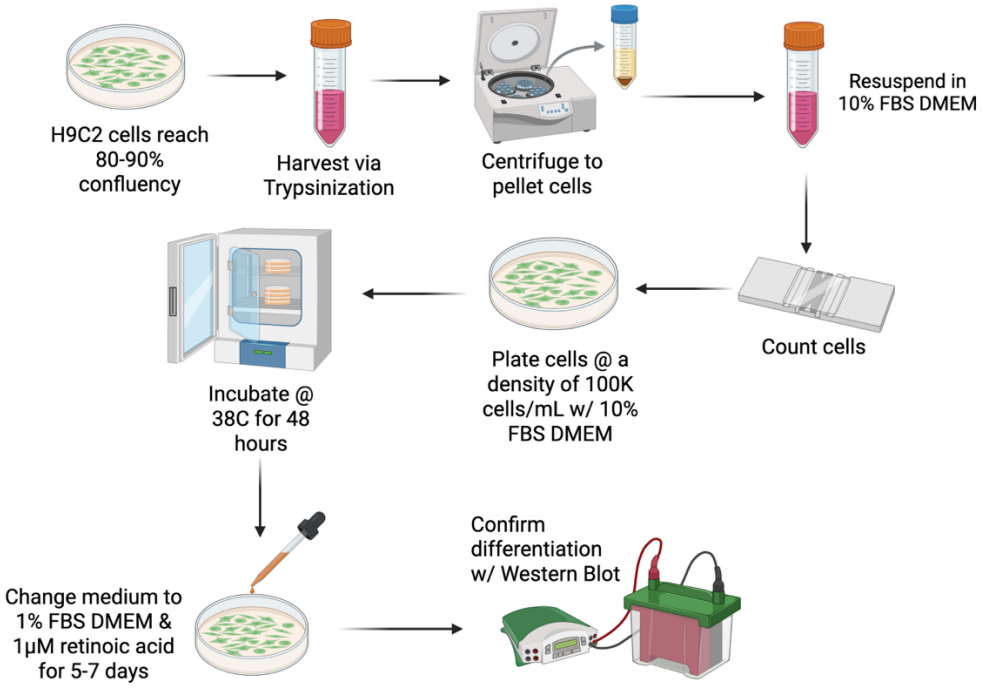

Figure 9: Differentiation Process of H9C2 cells into Cardio myoblasts.
Created in BioRender. Billings, T. (2025) https://BioRender.com/hy5k14m

ELISA method for determination for mitochondrial RNA N1 methylation

Mitochondria were isolated from H9C2 cells after ISO or control treatment. RNA was purified from the isolated mitochondria and secondary structure removed by incubating at 95°C for 5 minutes. RNA was digested by nuclease P1 then incubated with alkaline phosphatase and m1A levels determined by competitive ELISA.

Complex IV activity assay

Enzymatic activity of cytochrome C oxidase (complex IV) was determined using frozen heart tissue that was previously harvested as mentioned above. First, 25 mg of cardiac tissue was homogenized at 4ºC in 50 mM potassium phosphate buffer containing 1 mM EDTA and 0.1% Triton X-100. The samples were incubated on ice for 30 minutes then centrifuged at 10,000 g for 10 minutes at 4ºC and the protein concentration was collected. The enzymatic activity of complex IV was analyzed in 50 mM potassium phosphate buffer as described in a previously published method[57].

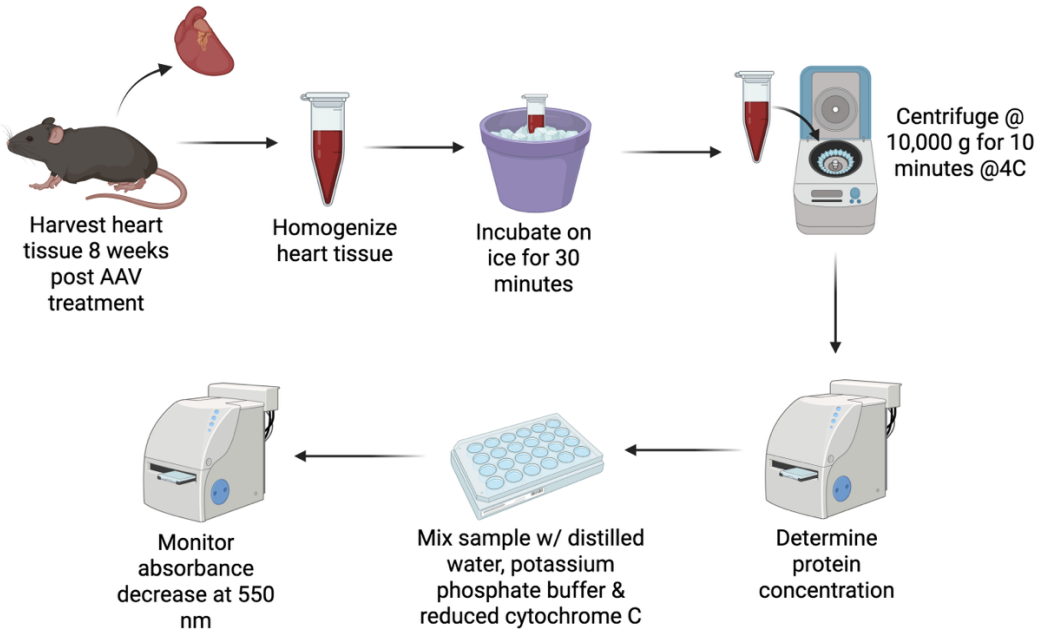

Figure 10: Complex IV Activity Assay Workflow.
Created in BioRender. Billings, T. (2025) https://BioRender.com/io1vntf

RNAiMAX Transfection Procedure

Differentiated H9C2 cells were plated in a 24-well plate at a confluency of 60-80% (0.5-1x10^5 cells) in serum free DMEM. After 24 hours, the lipofectamine and siRNA complex was mixed. First, 50 µl of Opti-MEM® medium and 1.5 µl of Lipofectamine® RNAiMAX reagent were mixed. Next, 50 µl and 1 µl of the siRNA were mixed. The diluted siRNA and diluted Lipofectamine® RNAiMAX were mixed in a 1:1 ratio and incubated for 5 minutes at room temperature. Finally, 25 u µl of the siRNA-lipid complex was added to each well and the plat incubated for 24 hours before analysis took place. The siRNAs used were the ambion® by life technologies *HSD17B10* Silencer® pre-designed silencing RNA and the ambion® by life technologies Negative control Silencer® pre-designed silencing RNA. These acted as the experimental and negative controls respectively.

Statistical Analysis

All data are presented as ± SEM. Statistical analysis was performed using GraphPad Prism 8.3 (GraphPad Software, Sand Diego, CA). Normal distribution of data was analyzed using a Shapiro-Wilk test. Comparisons between 3 or more groups were conducted by 1-way or 2-way ANOVA followed by a Tukey post hoc analysis. Comparison between 2 groups was done by using an unpaired, 2-tailed t test. All results were tested with the $P<0,05$ significance.

Results

Isoproterenol induced cardiomyocyte hypertrophy suppresses *Hsd17b10* gene expression and mitochondrial RNase P activity

To determine if the expression of the gene that encodes Mrpp2 is suppressed in cardiac hypertrophy, we used cardiomyocytes derived from H9c2 rat myoblasts and incubated them in 100 μM of isoproterenol (ISO) for 24 hours to induce a cardiac hypertrophic model. We utilized rtpcr analysis on extracted RNA to determine expression levels of *Hsd17b10,* the gene that encodes Mrpp2. Expression levels of known markers of cardiac hypertrophy *Nppa* and *Nppb* were elevated in the ISO treated samples in comparison to control (Figure 5A). Expression of *Serca2* which is known to decrease in pathologic cardiac hypertrophy was suppressed in our model[58]. The results suggested to us that the differentiated H9c2 cells developed pathologic hypertrophy with the ISO treatments. Expression of *Hsd17b10* was significantly downregulated in ISO treated cells in comparison to controls (Figure 5B). Finally, we determined the levels of N^1 adenosine methylation (m^1A) on extracted mitochondrial RNA. The N^1 methylation modification is catalyzed by the Mrpp1 subunit of the mitochondrial RNase P and is a marker of its catalytic activity. It has previously been shown that Mrpp2 binding to Mrpp1 is required for the m^1A reaction to be catalyzed[42]. We found mitochondrial RNA m^1A levels to be significantly down in the ISO treated cardiomyocytes in comparison to the control (Figure 5C). The results suggest to us that downregulation of the *Hsd17b10* gene in pathologic cardiac hypertrophy can disrupt RNase P catalysis. We, therefore, hypothesized that overexpression of the *Hsd17b10* gene would blunt the progression of pathologic cardiac hypertrophy to heart failure. We decided to test our hypothesis in more clinically relevant model of pathologic cardiac hypertrophy; the chronic pressure overload mouse model of transverse aortic constriction (TAC).

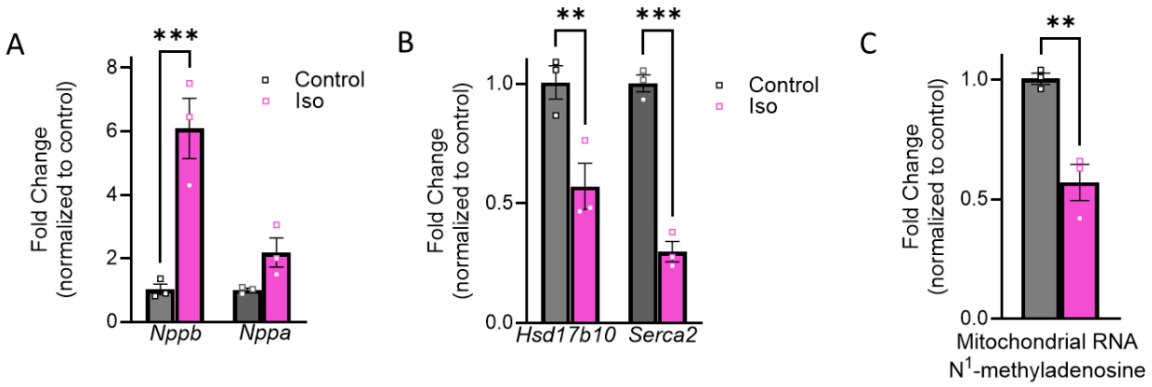

Figure 11: Isoproterenol induces cardiomyocyte hypertrophy that suppresses *HSD17B10* gene expression. (A) H9c2 cells were incubated with ISO (100μM) for 48 hours and RNA extracted for real-time PCR analysis. The mRNA expression levels of *Nppb, Nppa* and **(B)** *HSD17B10* and *Serca2* were determined by real-time PCR analysis normalized to *Gapdh*. (C)Mitochondrial RNA N^1-methyladenosine levels determined after ISO treatment. All data are presented as mean±SEM. P values were determined by one-way ANOVA followed by Tukey multiple comparison test. * $p < 0.05$ vs. controls.

Mrpp2 treatment helps to restore cardiac function and mitochondrial protein synthesis

To test if overexpression of the *Hsd17b10* gene would blunt the progression of heart failure, we sought to increase the expression of Mrpp2 in the myocardium of mice via retro-orbital injection of an adeno-associated virus serotype 9 vector carrying Mrpp2 directed by the cardiac-specific chicken troponin T (cTNT) promoter (AAV9.cTNT.Mrpp2). Therefore, we injected AAV9.cTNT.Mrpp2 virus or a control AAV9 carrying green fluorescent protein (GFP) (AAV9.cTNT.GFP) to mice 1 week after sham or transverse aortic constriction (TAC) surgery at a dosage of 1×10^{12} virus genomes per animal by retro-orbital injection. After 8 weeks, we performed echocardiography and harvested tissue for further analysis (Figure 6A). Our findings revealed a significant decrease in the expression of Mrpp2 in the TAC AAV9.cTNT.GFP treated hearts (Figure 6B & 6C) compared to Shams. Heart weight to body ratio and lung edema were increased while echocardiography revealed decreases in fractional shortening % (FS%) compared to Shams (Figure 6D & 6F). *Nppa* gene expression was found to be up in the GFP treated TAC models with reductions in Mrpp2 protein level and impaired mitochondrial RNase P

activity (Figure 7B). Taken together, the mice treated with the AAV9.cTNT.GFP developed pathologic cardiac hypertrophy, mitochondrial dysfunction, and heart failure. We found the AAV.cTNT.Mrpp2 treatment to robustly increase *Hsd17b10* levels in failing hearts (Figure 7A). Restoration of Mrpp2 levels enhanced RNase P activity, improved mtRNA processing, and blunted the progression of heart failure. Decreases in lung edema, pathologic hypertrophy, and increases in systolic heart function were found in mice that received AAV.cTNT.Mrpp2 compared to the control AAV.cTNT.GFP (Figure 6E-6G).

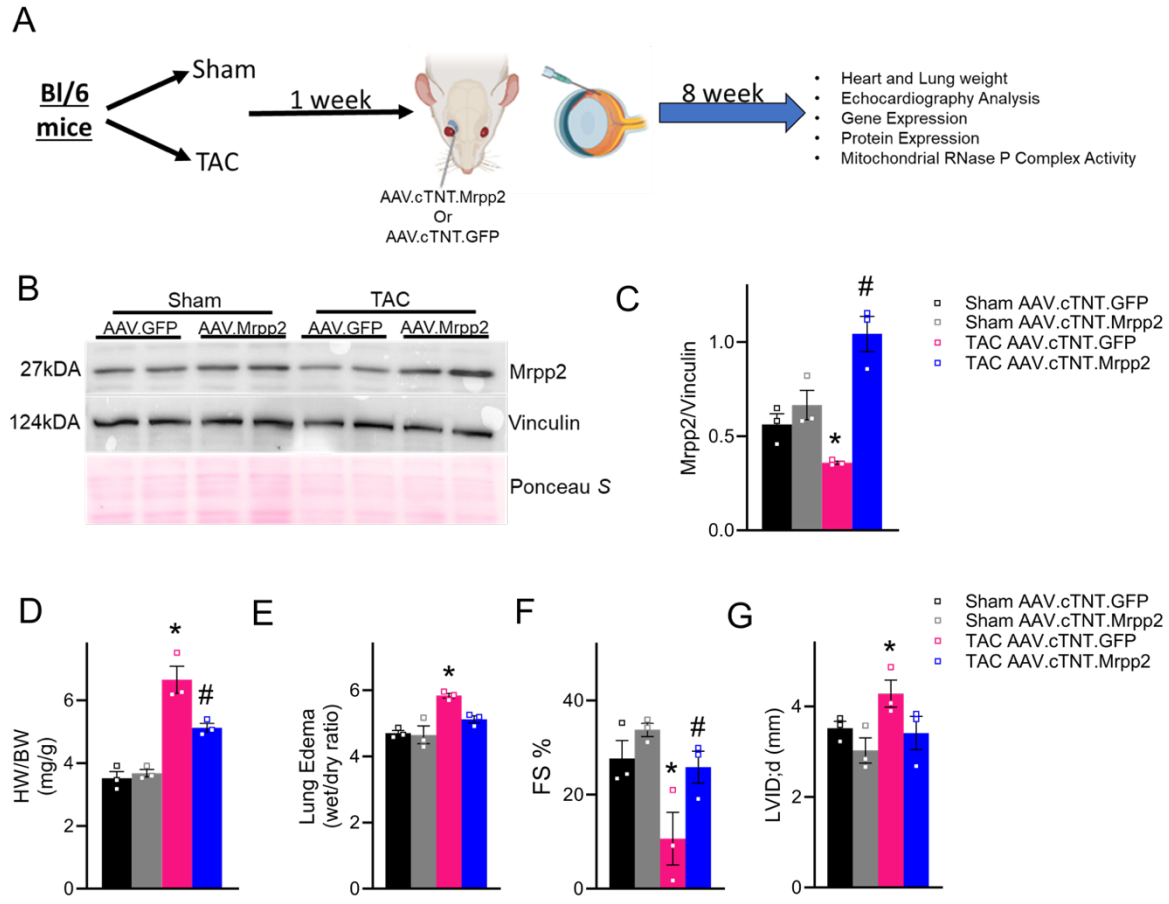

Figure 12: Mrpp2 treatment helps to restore cardiac function. (A) Experimental diagram and time points. Male Bl/6 mice underwent either SHAM/TAC surgery and after 1 week were treated with either AAV.cTNT.GFP or AAV.cTNT. Mrpp2 and after 8 weeks were analyzed. (B&C) Western blot data showing Mrpp2 protein expression in experimental groups. Protein was normalized to vinculin. (D) Heart weight to body weight ratio (HW/BW); n=3 mice per group. (E) Wet/Dry ratio of lung tissues (Lung Edema); n=3 mice per group. (F) Fractional shortening percentage (FS%); n=3 mice per group. (D) Left Ventricular Internal Diameter at end-diastole (LVID:d); n=3 mice per group, All data are presented as mean±SEM.

Nppa gene expression was lower in the AAV.cTNT.Mrpp2 treated TAC models (Figure 7B). Levels of Nd1:Nd2 expression were lowered in AAV.cTNT.Mrpp2 treated TAC models compared to the control AAV.cTNT.GFP indicating enhanced processing within the mitochondrial genome of the AAV.cTNT.Mrpp2 treated TAC models (Figure 7C). Levels of Mt-Nd1 and complex IV were restored indicating improvements in mitochondrial function. (Figure 7D-7F).

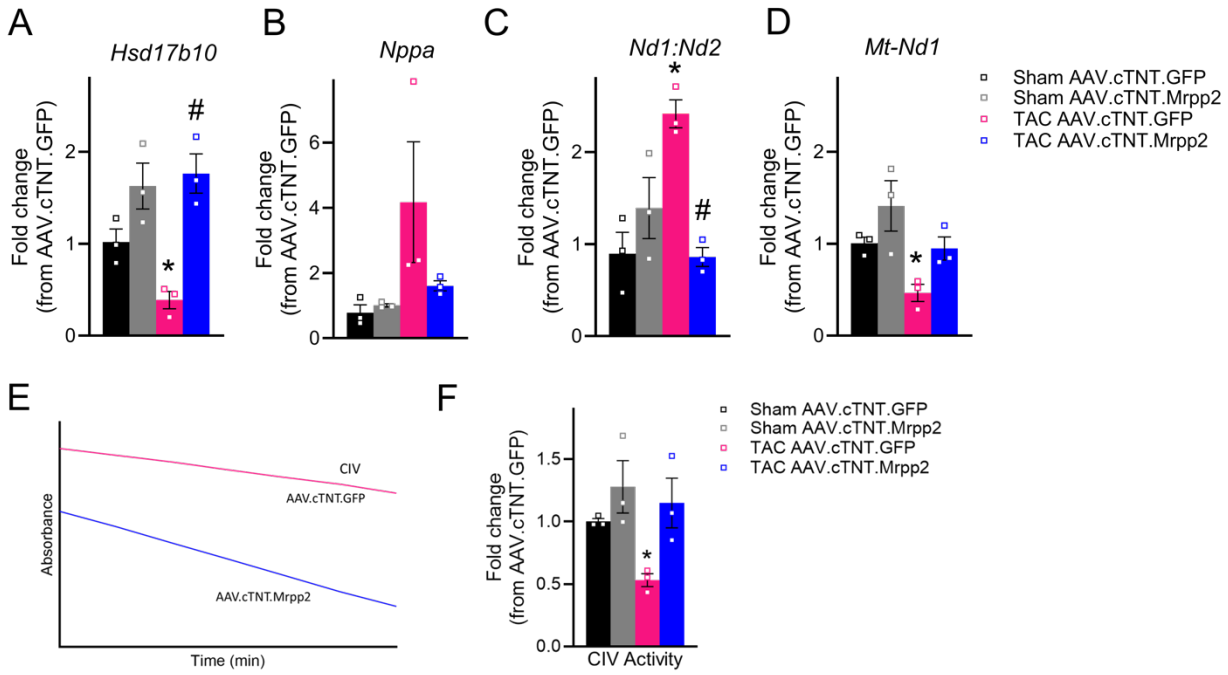

Figure 13: Mrpp2 restoration reduces cardiac hypertrophy and restores mitochondrial protein synthesis. (A) mRNA expression levels of HSD17B10. (B) mRNA expression levels of Nppa. (C) mRNA expression levels of Nd1:Nd:2. (D) mRNA expression levels of Mt-Nd1. All data was collected via cardiac tissue that was extracted from mouse models and RNA extracted for real-time PCR analysis. (E) Absorbance levels from activity assay of CIV. (F) CIV activity relative to control vector. N=3 mice per group. All data are presented as mean±SEM.

Discussion

We demonstrate in various models of pathologic cardiac hypertrophy and heart failure that the *Hsd17b10* gene is downregulated which correlates with impaired mitochondrial RNase P activity. Restoring Mrpp2 levels with our gene therapy in TAC hearts allowed us to determine the cause-effect relationship between Mrpp2 downregulation and mitochondrial dysfunction/heart failure. Our evidence suggests that disruption in the expression of *Hsd17b10* gene causes impaired function of mitochondrial RNase P splicing complex. Impaired RNase P in failing heart results in accumulation of immature mitochondrial RNA and reduced translation of the 13 ETC subunits encoded by the mtDNA. The evidence points to a dysregulation of the translation of the mitochondrial proteome that is intrinsic to mitochondria. By using the ISO induced pathologic cardiac hypertrophy model in differentiated H9c2 cells, we were able to demonstrate the pathologic hypertrophy induces downregulation of the *Hsd17b10* gene and impairs RNase P activity in mitochondria as indicated by decreased mitochondrial RNA m^1A levels. By using AAV9 directed gene therapy *in vivo* we were able to effectively restore mitochondrial RNase P activity and blunt the progression of heart failure in the TAC mouse model. Expression levels of the uncleaved Nd1:Nd2 transcript being high in the GFP treated TAC models indicates that improper processing of the mitochondrial polycistronic RNAs are taking place. Our evidence indicates this is insufficient to translate the mitochondrial genome to protein. With the treatment of an AAV9 carrying the *Hsd17b10* gene to TAC models, we were able to effectively lower the symptoms of cardiac hypertrophy. This indicates that the overexpression of the *Hsd17b10* gene specifically in cardiac muscle helps the post-transcriptional processing steps of mitochondrial genome and that tRNAs were cleaved at a higher rate than in TAC control models. There was also a downregulation of the NADH

dehydrogenase subunit 1 (Mt-Nd1) gene in the GFP treated TAC models which indicates a lowered expression of a mtDNA encoded subunit of ETC complex I. The level of Mt-Nd1 was restored to normal levels in the AAV9.cTNT.Mrpp2 treated TAC models. Finally, activity levels of complex IV were lowered in the GFP treated TAC models which indicates a lowered activity likely due to the absence of crucial complex IV proteins needed for proper activity within the respiratory chain. The AAV9.cTNT.Mrpp2 treated TAC models were able to restore activity in complex IV which indicates that AAV9.cTNT.Mrpp1 treatment was effective mtDNA encoded protein.

There were limitations to the study that are worth noting. First, the study had a small number of mice which reduces statistical power and making results not as reliable as they would be in a higher sample size cohort. Preliminary results show that AAV9.cTNT.Mrpp2 administration into cardiac tissue serves as a promising therapy in failing heart, however, it is necessary to include a larger cohort before drawing a strict conclusion. We also did not include any females in the study which is necessary to rule out any sex differences in treatment. Although we did not detect any toxicity with the gene therapy more work is required to completely rule out any unwanted side effects.

Future work could be done on this study to further improve the reliability of the results from the murine study. The study could first be redone with a larger cohort of mice along with a diverse set of male and female mice to account for sex differences as well as a longer timeframe of treatment to determine unwanted side effects. It would also be necessary to look at the gene expression and the enzymatic activity of all subunits of the ETC to see how mrpp2 treatment affects all enzymatic subunits of the ETC. Finally, investigations of gene therapy in diseases

such as HSD10 disease using transgenic mouse models would be a valuable next step in determining how well this gene therapy could treat genetic diseases leading to heart failure.

Conclusion

Our results support the idea that the *Hsd17b10* gene is crucial for the overall cardiac health of an individual. It is well known that when the gene expression is down, the critical RNase P subunit Mrpp2 is missing from RNase P splicing complex, resulting incomplete processing of the mtRNA transcript[34]. Our work with our hypertrophic cell model supported this statement by showing reduced mtRNA processing due to reduced RNaseP activity. The improper processing of the mitochondrial genome is detrimental to oxidative metabolism need for heart function and can lead to cardiac hypertrophy due to the energy imbalance caused by the damaged mitochondria. Once we demonstrated that the *Hsd17b10* gene was down in the hypertrophic models, we were able to support the hypothesis that overexpressing Hsd17b10 in the heart failure models would help restore cardiac function. We were able to use SHAM/TAC mouse models to show that recuing cardiac activity with the administration of the Mrpp2 gene into cardiac tissue may be an effective therapy in helping to restore cardiac function of patients experiencing cardiac hypertrophy.

References

[1] F. V. Sonics. "Guide to Small Animal Basic Echocardiography using the Vevo Ultrasound Systems." https://www.visualsonics.com/sites/default/files/MKT03791%20Guide%20to%20Basic%20Echocardiography%20Rev%201.0.pdf (accessed.

[2] G. D. Lopaschuk, Q. G. Karwi, R. Tian, A. R. Wende, and E. D. Abel, "Cardiac Energy Metabolism in Heart Failure," (in eng), *Circ Res,* vol. 128, no. 10, pp. 1487-1513, May 14 2021, doi: 10.1161/CIRCRESAHA.121.318241.

[3] Z. Arany and U. Elkayam, "Peripartum Cardiomyopathy," vol. 133, ed, 2016.

[4] E. Clark *et al.*, "Role of frataxin protein deficiency and metabolic dysfunction in Friedreich ataxia, an autosomal recessive mitochondrial disease," (in eng), *Neuronal Signal,* vol. 2, no. 4, p. NS20180060, Dec 2018, doi: 10.1042/NS20180060.

[5] J. Ritterhoff and R. Tian, "Metabolic mechanisms in physiological and pathological cardiac hypertrophy: new paradigms and challenges," (in eng), *Nat Rev Cardiol,* vol. 20, no. 12, pp. 812-829, Dec 2023, doi: 10.1038/s41569-023-00887-x.

[6] S. C. K. Jr, S. Purohit, and R. Tian, "Cardiac Metabolism and Its Interactions with Contraction, Growth, and Survival of the Cardiomyocte," ed, 2013.

[7] S. Neubauer, "The failing heart--an engine out of fuel," (in eng), *N Engl J Med,* vol. 356, no. 11, pp. 1140-51, Mar 15 2007, doi: 10.1056/NEJMra063052.

[8] J. S. Ingwall and R. G. Weiss, "Is the Failing Heart Energy Starved?," *Circulation Research,* vol. 95, no. 2, pp. 135-145, 2004, doi: doi:10.1161/01.RES.0000137170.41939.d9.

[9] G. Karamanlidis, L. Nascimben, G. S. Couper, P. S. Shekar, F. del Monte, and R. Tian, "Defective DNA replication impairs mitochondrial biogenesis in human failing hearts," (in eng), *Circ Res,* vol. 106, no. 9, pp. 1541-8, May 14 2010, doi: 10.1161/CIRCRESAHA.109.212753.

[10] G. Karamanlidis, L. Garcia-Menendez, S. C. Kolwicz, C. F. Lee, and R. Tian, "Promoting PGC-1α-driven mitochondrial biogenesis is detrimental in pressure-overloaded mouse hearts," (in eng), *Am J Physiol Heart Circ Physiol,* vol. 307, no. 9, pp. H1307-16, Nov 01 2014, doi: 10.1152/ajpheart.00280.2014.

[11] M. A. Walker *et al.*, "Raising NAD," (in eng), *Circulation,* vol. 148, no. 25, pp. 2038-2057, Dec 19 2023, doi: 10.1161/CIRCULATIONAHA.123.066039.

[12] G. Karamanlidis *et al.*, "Mitochondrial complex I deficiency increases protein acetylation and accelerates heart failure," (in eng), *Cell Metab,* vol. 18, no. 2, pp. 239-50, Aug 06 2013, doi: 10.1016/j.cmet.2013.07.002.

[13] C. F. Lee *et al.*, "Normalization of NAD+ Redox Balance as a Therapy for Heart Failure," (in eng), *Circulation,* vol. 134, no. 12, pp. 883-94, Sep 20 2016, doi: 10.1161/CIRCULATIONAHA.116.022495.

[14] B. Zhou and R. Tian, "Mitochondrial dysfunction in pathophysiology of heart failure," ed, 2018.

[15] A. B, J. A, L. J, and e. al, *The Mitochondrion* (Molecular Biology of the Cell. 4th edition). New York: Garland Science, 2002.

[16] Luigino Nascimben *et al.*, "Mechanisms for Increased Glycolysis in the Hypertrophied Rat Heart," vol. 44, ed, 2004.

[17] Gary D. Lopaschuk , John R. Ussher , Clifford D. L. Folmes , J. S. Jaswal, and W. C. Stanley, "Myocardial Fatty Acid Metabolism in Health and Disease," ed, 2010.
[18] D. C. Logan, "The mitochondrial compartment," (in eng), *J Exp Bot,* vol. 58, no. 1, pp. 1225-43, 2007.
[19] C. A. Mannella, W. J. Lederer, and M. S. Jafri, "The connection between inner membrane topology and mitochondrial function," (in eng), *J Mol Cell Cardiol,* vol. 62, pp. 51-7, Sep 2013, doi: 10.1016/j.yjmcc.2013.05.001.
[20] D. Nolfi-Donegan, A. Braganza, and S. Shiva, "Mitochondrial electron transport chain: Oxidative phosphorylation, oxidant production, and methods of measurement," (in eng), *Redox Biol,* vol. 37, p. 101674, Oct 2020, doi: 10.1016/j.redox.2020.101674.
[21] C. Yan, X. Duanmu, L. Zeng, B. Liu, and Z. Song, "Mitochondrial DNA: Distribution, Mutations, and Elimination," (in eng), *Cells,* vol. 8, no. 4, Apr 25 2019, doi: 10.3390/cells8040379.
[22] I. Martínez-Reyes and N. S. Chandel, "Mitochondrial TCA cycle metabolites control physiology and disease," (in eng), *Nat Commun,* vol. 11, no. 1, p. 102, Jan 03 2020, doi: 10.1038/s41467-019-13668-3.
[23] R. N. Lightowlers, A. Rozanska, and Z. M. Chrzanowska-Lightowlers, "Mitochondrial protein synthesis: figuring the fundamentals, complexities and complications, of mammalian mitochondrial translation," (in eng), *FEBS Lett,* vol. 588, no. 15, pp. 2496-503, Aug 01 2014, doi: 10.1016/j.febslet.2014.05.054.
[24] B. R. Walker and C. T. Moraes, "Nuclear-Mitochondrial Interactions," (in eng), *Biomolecules,* vol. 12, no. 3, Mar 10 2022, doi: 10.3390/biom12030427.
[25] S. R. Bacman, P. A. Gammage, M. Minczuk, and C. T. Moraes, *Manipulation of mitochondrial genes and mtDNA heteroplasmy*. Academic Press, 2020.
[26] A. R. D'Souza and M. Minczuk, "Mitochondrial transcription and translation: overview," (in eng), *Essays Biochem,* vol. 62, no. 3, pp. 309-320, Jul 20 2018, doi: 10.1042/EBC20170102.
[27] K. E. Guja and M. Garcia-Diaz, "Hitting the brakes: Termination of mitochondrial transcription," *Biochimica et Biophysica Acta (BBA) - Gene Regulatory Mechanisms,* vol. 1819, no. 9-10, pp. 939-947, 2011.
[28] E. Bouda, A. Stapon, and M. Garcia-Diaz, "Mechanisms of mammalian mitochondrial transcription," (in eng), *Protein Sci,* vol. 28, no. 9, pp. 1594-1605, Sep 2019, doi: 10.1002/pro.3688.
[29] F. Wang, D. Zhang, P. Li, and Y. Gao, "Mitochondrial Protein Translation: Emerging Roles and Clinical Significance in Disease," (in eng), *Front Cell Dev Biol,* vol. 9, p. 675465, 2021, doi: 10.3389/fcell.2021.675465.
[30] T. R. Mercer *et al.*, "The human mitochondrial transcriptome," (in eng), *Cell,* vol. 146, no. 4, pp. 645-58, Aug 19 2011, doi: 10.1016/j.cell.2011.06.051.
[31] J. W. Taanman, "The mitochondrial genome: structure, transcription, translation and replication," (in eng), *Biochim Biophys Acta,* vol. 1410, no. 2, pp. 103-23, Feb 09 1999, doi: 10.1016/s0005-2728(98)00161-3.
[32] M. Jedynak-Slyvka, A. Jabczynska, and R. J. Szczesny, "Human Mitochondrial RNA Processing and Modifications: Overview," (in eng), *Int J Mol Sci,* vol. 22, no. 15, Jul 27 2021, doi: 10.3390/ijms22157999.

[33] A. V. Kotrys and R. J. Szczesny, "Mitochondrial Gene Expression and Beyond-Novel Aspects of Cellular Physiology," (in eng), *Cells,* vol. 9, no. 1, Dec 19 2019, doi: 10.3390/cells9010017.
[34] M. Saoji, A. Sen, and R. T. Cox, "Loss of Individual Mitochondrial Ribonuclease P Complex Proteins Differentially Affects Mitochondrial tRNA Processing In Vivo," (in eng), *Int J Mol Sci,* vol. 22, no. 11, Jun 04 2021, doi: 10.3390/ijms22116066.
[35] H. Betat, Y. Long, J. E. Jackman, and M. Mörl, "From end to end: tRNA editing at 5'- and 3'-terminal positions," (in eng), *Int J Mol Sci,* vol. 15, no. 12, pp. 23975-98, Dec 22 2014, doi: 10.3390/ijms151223975.
[36] K. Kerkhofs *et al.*, "Altered tRNA processing is linked to a distinct and unusual La protein in Tetrahymena thermophila," (in eng), *Nat Commun,* vol. 13, no. 1, p. 7332, Nov 28 2022, doi: 10.1038/s41467-022-34796-3.
[37] S. Liao, L. Chen, Z. Song, and H. He, "The fate of damaged mitochondrial DNA in the cell," (in eng), *Biochim Biophys Acta Mol Cell Res,* vol. 1869, no. 5, p. 119233, May 2022, doi: 10.1016/j.bbamcr.2022.119233.
[38] A. Sen, A. Karasik, A. Shanmuganathan, E. Mirkovic, M. Koutmos, and R. T. Cox, "Loss of the mitochondrial protein-only ribonuclease P complex causes aberrant tRNA processing and lethality in Drosophila," (in eng), *Nucleic Acids Res,* vol. 44, no. 13, pp. 6409-22, Jul 27 2016, doi: 10.1093/nar/gkw338.
[39] S. C. Walker and D. R. Engelke, "A protein-only RNase P in human mitochondria," (in eng), *Cell,* vol. 135, no. 3, pp. 412-4, Oct 31 2008, doi: 10.1016/j.cell.2008.10.010.
[40] A. Bhatta, C. Dienemann, P. Cramer, and H. S. Hillen, "Structural basis of RNA processing by human mitochondrial RNase P," *Nat Struct Mol Biol,* vol. 28, pp. 713-723, 2021, doi: https://doi.org/10.1038/s41594-021-00637-y.
[41] B. K. Mohanty and S. R. Kushner, "Inactivation of RNase P in Escherichia coli significantly changes post-transcriptional RNA metabolism," (in eng), *Mol Microbiol,* vol. 117, no. 1, pp. 121-142, Jan 2022, doi: 10.1111/mmi.14808.
[42] S. Oerum *et al.*, "Structural insight into the human mitochondrial tRNA purine N1-methyltransferase and ribonuclease P complexes," (in eng), *J Biol Chem,* vol. 293, no. 33, pp. 12862-12876, Aug 17 2018, doi: 10.1074/jbc.RA117.001286.
[43] M. Saoji and R. T. Cox, "Mitochondrial RNase P Complex in Animals: Mitochondrial tRNA Processing and Links to Disease.," vol. 34, ed. Springer, 2018.
[44] P. Bénit *et al.*, "Mutant NDUFV2 subunit of mitochondrial complex I causes early onset hypertrophic cardiomyopathy and encephalopathy," (in eng), *Hum Mutat,* vol. 21, no. 6, pp. 582-6, Jun 2003, doi: 10.1002/humu.10225.
[45] M. D. Metodiev *et al.*, "Recessive Mutations in TRMT10C Cause Defects in Mitochondrial RNA Processing and Multiple Respiratory Chain Deficiencies," (in eng), *Am J Hum Genet,* vol. 99, no. 1, p. 246, Jul 07 2016, doi: 10.1016/j.ajhg.2016.06.013.
[46] L. Wang, L. He, B. Zhou, K. Li, and X. Liu, "Clinical Presentation of Combined Oxidative Phosphorylation Deficiency 30 (COXPD30) & mutations in the TRMT10C gene," (in eng), *QJM,* Jan 02 2025, doi: 10.1093/qjmed/hcae251.
[47] S. Oerum *et al.*, "Novel patient missense mutations in the HSD17B10 gene affect dehydrogenase and mitochondrial tRNA modification functions of the encoded protein," (in eng), *Biochim Biophys Acta Mol Basis Dis,* vol. 1863, no. 12, pp. 3294-3302, Dec 2017, doi: 10.1016/j.bbadis.2017.09.002.

[48] Z. J, "HSD10 disease: clinical consequences of mutations in the HSD17B10 gene," *J Inherit Metab Dis,* 2012, doi: 10.1007/s10545-011-9415-4.
[49] I. Hochberg *et al.*, "Bi-allelic variants in the mitochondrial RNase P subunit PRORP cause mitochondrial tRNA processing defects and pleiotropic multisystem presentations," (in eng), *Am J Hum Genet,* vol. 108, no. 11, pp. 2195-2204, Nov 04 2021, doi: 10.1016/j.ajhg.2021.10.002.
[50] C. D. Porada, C. Stem, and G. Almeida-Porada, "Gene therapy: the promise of a permanent cure," (in eng), *N C Med J,* vol. 74, no. 6, pp. 526-9, Nov-Dec 2013.
[51] M. F. Naso, B. Tomkowicz, W. L. Perry, and W. R. Strohl, "Adeno-Associated Virus (AAV) as a Vector for Gene Therapy," (in eng), *BioDrugs,* vol. 31, no. 4, pp. 317-334, Aug 2017, doi: 10.1007/s40259-017-0234-5.
[52] J. M. Riyad and T. Weber, "Intracellular trafficking of adeno-associated virus (AAV) vectors: challenges and future directions," (in eng), *Gene Ther,* vol. 28, no. 12, pp. 683-696, Dec 2021, doi: 10.1038/s41434-021-00243-z.
[53] H. Zhang, Q. Zhan, B. Huang, Y. Wang, and X. Wang, "AAV-mediated gene therapy: Advancing cardiovascular disease treatment," (in eng), *Front Cardiovasc Med,* vol. 9, p. 952755, 2022, doi: 10.3389/fcvm.2022.952755.
[54] M. A. DiMattia *et al.*, "Structural insight into the unique properties of adeno-associated virus serotype 9," (in eng), *J Virol,* vol. 86, no. 12, pp. 6947-58, Jun 2012, doi: 10.1128/JVI.07232-11.
[55] Y. Kim, A. P. Landstrom, S. H. Shah, J. C. Wu, C. E. Seidman, and o. b. o. t. A. H. Association, "Gene Therapy in Cardiovascular Disease: Recent Advances and Future Directions in Science: A Science Advisory From the American Heart Association," *Circulation,* vol. 150, no. 23, pp. e471-e480, 2024, doi: doi:10.1161/CIR.0000000000001296.
[56] K. Zsebo *et al.*, "Long-Term Effects of AAV1/SERCA2a Gene Transfer in Patients With Severe Heart Failure," *Circulation Research,* vol. 114, no. 1, pp. 101-108, 2014, doi: doi:10.1161/CIRCRESAHA.113.302421.
[57] M. Spinazzi, A. Casarin, V. Pertegato, L. Salviati, and C. Angelini, "Assessment of mitochondrial respiratory chain enzymatic activities on tissues and cultured cells."
[58] T. Takizawa, M. Arai, A. Yoguchi, K. Tomaru, M. Kurabayashi, and R. Nagai, "Transcription of the SERCA2 gene is decreased in pressure-overloaded hearts: A study using in vivo direct gene transfer into living myocardium," (in eng), *J Mol Cell Cardiol,* vol. 31, no. 12, pp. 2167-74, Dec 1999, doi: 10.1006/jmcc.1999.1045.